Article

Cell Reports

Cytosolic Pellino-1-Mediated K63-Linked Ubiquitination of IRF5 in M1 Macrophages Regulates Glucose Intolerance in Obesity

Graphical Abstract

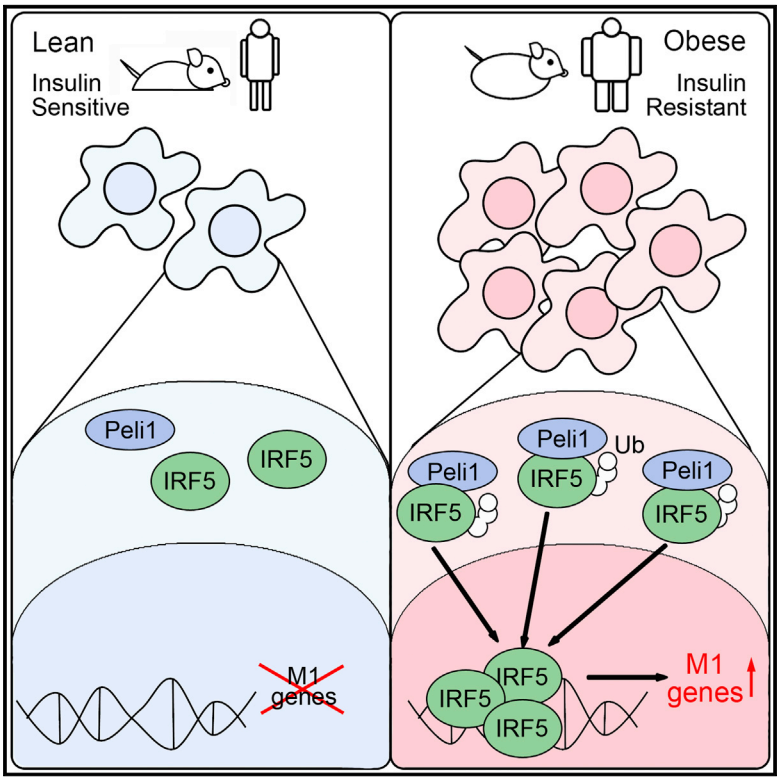

Authors

Donghyun Kim, Ho Lee, Jaemoon Koh, ..., Chang Woo Lee, Won-Woo Lee, Doo Hyun Chung

Correspondence

doohyun@snu.ac.kr

In Brief

Kim et al. demonstrate that ubiquitin E3 ligase Pellino-1 promotes macrophage M1 polarization and obesity-induced glucose intolerance in mice and humans. Furthermore, Pellino-1 induces nuclear translocation of IRF5 by binding and K63-linked ubiquitination.

Highlights

- Pellino-1 promotes macrophage M1 polarization
- Pellino-1 induces K63-dependent ubiquitination and nuclear translocation of IRF5
- Pellino-1 knockout mice show reduction of obesity and glucose intolerance
- Pellino-1 expression correlates with HOMA-IR and M1 macrophage in human

Kim et al., 2017, Cell Reports *20*, 832–845
July 25, 2017
http://dx.doi.org/10.1016/j.celrep.2017.06.088

OPEN ACCESS
CellPress

Cell Reports
Article

Cytosolic Pellino-1-Mediated K63-Linked Ubiquitination of IRF5 in M1 Macrophages Regulates Glucose Intolerance in Obesity

Donghyun Kim,[1,2,8] Ho Lee,[6,8] Jaemoon Koh,[1] Jae Sung Ko,[1,2] Bo Ruem Yoon,[3] Yoon Kyung Jeon,[1] Young Min Cho,[4] Tae Han Kim,[5] Yun-Suhk Suh,[5] Hyuk-Joon Lee,[5] Han-Kwang Yang,[5] Kyong Soo Park,[4] Hye Young Kim,[2] Chang Woo Lee,[7] Won-Woo Lee,[3] and Doo Hyun Chung[1,2,9,*]

[1]Department of Pathology, Seoul National University College of Medicine, Seoul 110-799, Korea
[2]Laboratory of Immune Regulation, Department of Biomedical Sciences, Seoul National University College of Medicine, Seoul 110-799, Korea
[3]Department of Microbiology and Immunology, Seoul National University College of Medicine, Seoul 110-799, Korea
[4]Department of Internal Medicine, Seoul National University College of Medicine, Seoul 110-799, Korea
[5]Department of Surgery and Cancer Research Institute, Seoul National University College of Medicine, Seoul 110-799, Korea
[6]Graduate School of Cancer Science and Policy, Research Institute, National Cancer Center, Goyang 10408, Korea
[7]Department of Molecular Cell Biology, Samsung Biomedical Research Institute, Sungkyunkwan University School of Medicine, Suwon 440-746, Korea
[8]These authors contributed equally
[9]Lead Contact
*Correspondence: doohyun@snu.ac.kr
http://dx.doi.org/10.1016/j.celrep.2017.06.088

SUMMARY

IRF5 is a signature transcription factor that induces M1 macrophage polarization. However, little is known regarding cytosolic proteins that induce IRF5 activation for M1 polarization. Here, we report the interaction between ubiquitin E3 ligase Pellino-1 and IRF5 in the cytoplasm, which increased nuclear translocation of IRF5 by K63-linked ubiquitination in human and mouse M1 macrophages. LPS and/or IFN-γ increased Pellino-1 expression, and M1 polarization was attenuated in Pellino-1-deficient macrophages in vitro and in vivo. Defective M1 polarization in Pellino-1-deficient macrophages improved glucose intolerance in mice fed a high-fat diet. Furthermore, macrophages in adipose tissues from obese humans exhibited increased Pellino-1 expression and IRF5 nuclear translocation compared with nonobese subjects, and these changes are associated with insulin resistance index. This study demonstrates that cytosolic Pellino-1-mediated K63-linked ubiquitination of IRF5 in M1 macrophages regulates glucose intolerance in obesity, suggesting a cytosolic mediator function of Pellino-1 in TLR4/IFN-γ receptor-IRF5 axis during M1 polarization.

INTRODUCTION

The Pellino protein was identified as a protein that interacts with the kinase domain of Pelle, the ortholog of the interleukin (IL)-1R-associated kinase in the Toll signaling pathway in *Drosophila melanogaster* (Grosshans et al., 1999). In mammalian systems, three isoforms—Pellino-1 (gene name: *PELI1* in human and *Peli1* in mouse), Pellino-2, and Pellino-3—have been reported to exert functions as ubiquitin E3 ligases (Jin et al., 2012; Moynagh, 2014). Structurally, the Pellino proteins contain a conserved RING-like domain at the C terminus that confers ubiquitin E3 ligase activity and a forkhead-associated (FHA) domain that interacts with target proteins, indicating that Pellino proteins share strong sequence homology and structural domains (Humphries and Moynagh, 2015). Several studies have shown that Pellino-1 plays essential roles in various innate and adaptive immune cells (Chang et al., 2009, 2011; Ordureau et al., 2008). In T cells, Pellino-1 inhibits T cell-receptor (TCR) signaling through K48-linked ubiquitination of c-Rel (Chang et al., 2011), inducing autoimmunity in Pellino-1-deficient mice. In contrast, Pellino-1 is critically involved in promoting Toll-like receptor 3 (TLR3)- and -4-mediated signals by interacting with IRAK1 and RIP1 in macrophages (Chang et al., 2009; Ordureau et al., 2008), suggesting that Pellino-1 might play pivotal roles in regulating immune responses in vivo by modulating macrophage functions.

Macrophages are heterogeneous and can be classified into several subsets. M1 (classically activated) and M2 (alternatively activated) macrophages represent two extreme dynamic activation states of macrophages (Murray et al., 2014). M1 macrophages promote inflammation by producing pro-inflammatory cytokines and reactive oxygen species, whereas M2 macrophages reduce inflammation but enhance the repair process in injured tissues by secreting anti-inflammatory cytokines (Lawrence and Natoli, 2011; Murray et al., 2014). Thus, the balance between M1 and M2 macrophage polarization is critical for regulating pathological processes in various diseases, including airway inflammation, arthritis, atherosclerosis, infection, cancer, and obesity-induced insulin resistance (Chawla et al., 2011; Lawrence and Natoli, 2011; Sica and Bronte, 2007; Sica and Mantovani, 2012). Several receptor-mediated signals and transcription factors have been well characterized as regulating M1-M2 macrophage polarization in different studies. M1 macrophages are polarized by Toll-like receptor 4 (TLR4) ligands and/or interferon (IFN)-γ, whereas M2 macrophages are polarized by

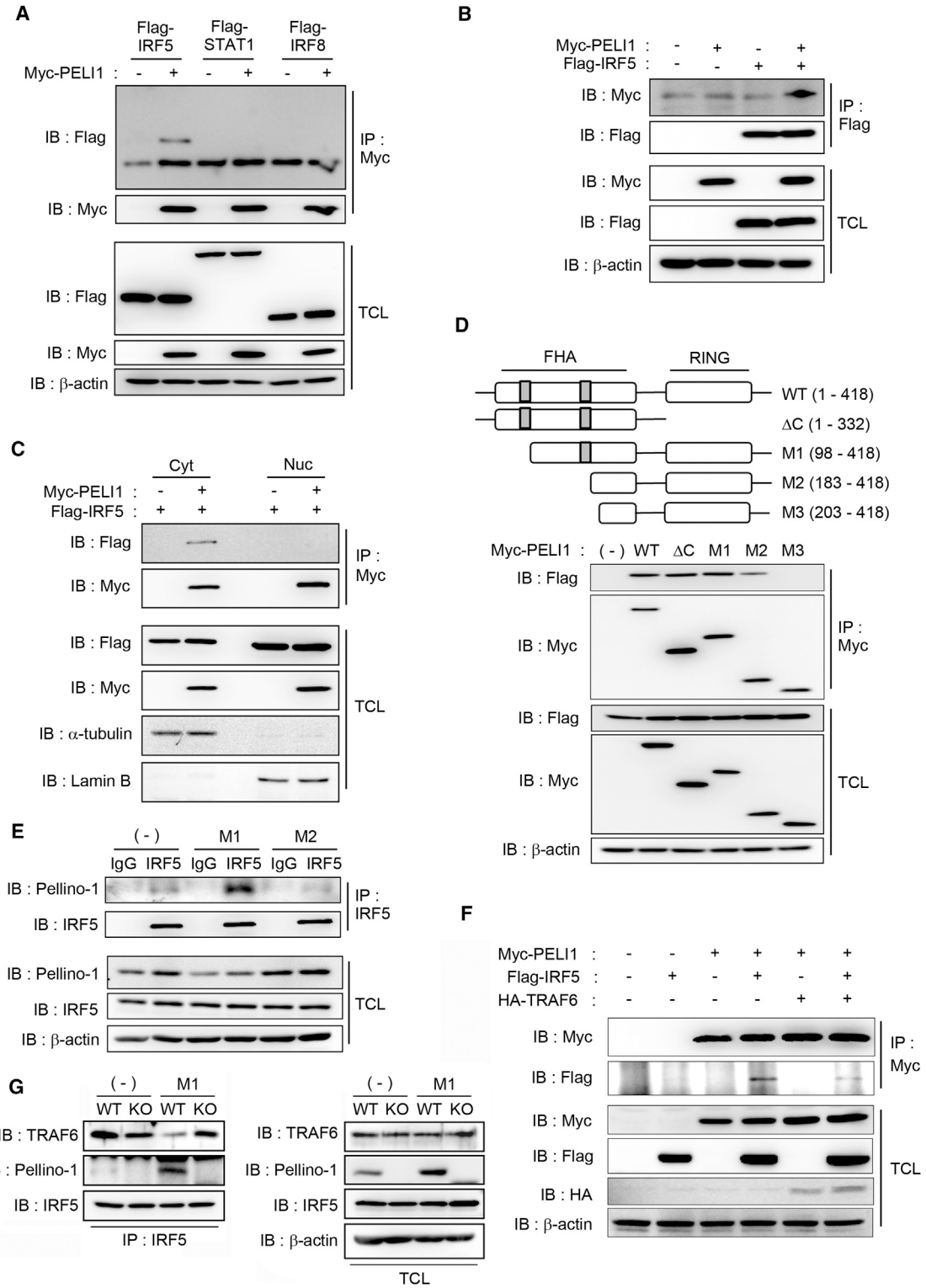

Figure 1. Pellino-1 Binds IRF5 during M1 Macrophage Polarization

(A) 293T cells were co-transfected with Myc-PELI1 and FLAG-IRF5, -STAT1, or -IRF8. Lysates from these cells were immunoprecipitated using an anti-Myc antibody and blotted with an anti-FLAG antibody.

(B) Lysates from 293T cells that were co-transfected with expression plasmids encoding Myc-*PELI1* and FLAG-*IRF5* were immunoprecipitated using an anti-FLAG antibody and immunoblotted with an anti-Myc antibody.

(legend continued on next page)

Th2 cytokines. Furthermore, it has been reported that interferon regulatory factor 5 (IRF5) is a signature transcription factor that promotes M1 macrophage polarization, whereas STAT6, STAT3, and IRF4 are critically involved in M2 polarization (Lawrence and Natoli, 2011; Murray et al., 2014). Moreover, it has been reported that IRF5 is activated by phosphorylation or ubiquitination, resulting in enhanced nuclear translocation and transcription factor activity (Balkhi et al., 2008; Ren et al., 2014). Thus, the identification and characterization of regulatory proteins that activate IRF5 via ubiquitination in M1 macrophages is critical for a comprehensive understanding of the M1 polarization mechanisms for diseases such as obesity-induced insulin resistance. However, little is known regarding the mechanism for ubiquitination-mediated IRF5 activation during M1 macrophage polarization. Here, we show that Pellino-1 directly bound and activated IRF5 via K63-linked ubiquitination upon TLR4 ligand and/or IFN-γ stimulation, thereby promoting M1 macrophage polarization and regulating glucose intolerance in obese humans and mice. Thus, this study reports the interaction of Pellino-1 and IRF5 in M1 macrophages, which regulates glucose intolerance in obesity, thereby suggesting a common cytosolic functional mediator of Pellino-1 in TLR4/IFN-γ receptor-IRF5 axis during M1 macrophage polarization.

RESULTS

Ubiquitin E3 Ligase Pellino-1 Induces K63-Linked Ubiquitination of IRF5 via Direct Interaction, Resulting in Enhancing the Nuclear Translocation and Activity of IRF5 in M1 Macrophages

We tested the binding between ubiquitin E3 ligase Pellino-1 and several transcription factors, including IRF5, to explore whether Pellino-1 directly interacts with IRF5 in M1 macrophage polarization (Figure 1A). Among these factors, IRF5 specifically bound Pellino-1 in transfected 293T cells (Figures 1A and 1B). The IRF5-Pellino-1 interaction was found in the cytosolic, but not the nuclear, fraction of 293T cells (Figure 1C), depending on amino acids 183–202 of Pellino-1 (Figure 1D). We immunoprecipitated IRF5 and immunoblotted Pellino-1 in M1- or M2-polarized bone-marrow-derived macrophages (BMDMs) to confirm the interaction between Pellino-1 and IRF5 in BMDMs, and these results revealed a specific interaction between IRF5 and Pellino-1 in M1-polarized BMDMs but not M2-polarized BMDMs (Figure 1E). Ubiquitin E3 ligase tumor necrosis factor (TNF)-receptor-associated factor (TRAF)6 was reported to interact with IRF5 in 293T cells (Balkhi et al., 2008), and co-transfection of TRAF6 inhibited the ability of Pellino-1 to bind IRF5 in 293T cells (Figure 1F), suggesting that Pellino-1 might compete with TRAF6 for binding of IRF5. Consistently, the IRF5-TRAF6 binding was increased in Pellino-1-deficient BMDMs compared with wild-type (WT) BMDMs (Figure 1G). Moreover, the IRF5-Pellino-1 interaction was increased in M1-polarized BMDMs, while IRF5-TRAF6 binding was reduced (Figure 1G). These findings indicate that K63-linked IRF5 ubiquitination is mediated by Pellino-1 rather than TRAF6 during M1 macrophage polarization.

Next, to investigate whether the interaction of Pellino-1 and IRF5 induces ubiquitination of IRF5, we estimated the poly-ubiquitination of IRF5 in 293T cells co-transfected with *PELI1* and *IRF5*. Pellino-1 induced the K63-linked ubiquitination of IRF5, in contrast to the K48-dependent mechanism, and this result was not obtained following transfection of Pellino-1 with a RING-domain deletion, a critical domain for E3 ligase function (Figure 2A). Moreover, denatured samples from co-transfected 293T cells and in vitro ubiquitination assay also demonstrated the poly-ubiquitination of IRF5 in the presence of Pellino-1 (Figures S1A and S1C). These results suggest that Pellino-1 might bind and induce K63-linked ubiquitination of IRF5 during M1 polarization of murine macrophages. Consistently, WT BMDMs showed more poly-ubiquitination of immunoprecipitated IRF5 upon M1 polarization compared with Pellino-1-deficient BMDMs in the absence or presence of denaturation of samples (Figures 2B and S1B). Considering IRF5 activation via ubiquitination-mediated nuclear translocation (Balkhi et al., 2008; Ren et al., 2014), we examined the nuclear translocation of IRF5 and Pellino-1 expression in cytosolic and nuclear fractions of BMDMs generated from WT and *Peli1*$^{-/-}$ mice. M1 stimulation increased the cytosolic and nuclear expression levels of Pellino-1 in BMDMs and human-monocyte-derived macrophages (HMDMs) (Figures 2C and 2D). In contrast to Pellino-1, the nuclear expression levels of IRF5 were increased in WT BMDMs and HMDMs upon M1 stimulation in a dose-dependent manner, whereas IRF5 expression was slightly reduced in the cytoplasm of BMDMs and HMDMs (Figures 2C, 2D, and S1D), indicating that the nuclear translocation of IRF5 was increased in BMDMs and HMDMs during M1 polarization. Moreover, the nuclear translocation of IRF5 in Pellino-1-deficient BMDMs and Pellino-1-knockdown HMDMs was less than that observed in WT BMDMs and HMDMs during M1 polarization. These findings suggest that Pellino-1 might enhance the translocation of IRF5 from the cytosol into the nucleus in M1-polarized BMDMs and HMDMs. Furthermore, a chromatin immunoprecipitation assay revealed that more IRF5 bound to the *Il12a* and *Nos2* promoters

(C) The cytosolic and nuclear fractions were isolated from 293T cells co-transfected with Myc-PELI1 and FLAG-IRF5 and were immunoprecipitated using an anti-Myc antibody and blotted with an anti-FLAG antibody.
(D) Diagram of the WT and mutant Pellino1 constructs (top). 293T cells were co-transfected with expression plasmids encoding Myc-*PELI1* and FLAG-*IRF5* WT; a RING-domain-deficient mutant (ΔC); or mutants 1(M1), 2 (M2), or 3 (M3) and were immunoprecipitated using anti-Myc antibody and immunoblotted with an anti-FLAG antibody (bottom).
(E) BMDMs from WT mice were simulated with M1 (IFN-γ + LPS) or M2 (IL-4 + IL-13) conditions for 30 min and harvested for immunoprecipitation with an anti-IRF5 antibody. These immunoprecipitated samples were immunoblotted for Pellino-1 or IRF5.
(F) 293T cells were co-transfected with Myc-PELI1, FLAG-IRF5, and hemagglutinin (HA)-TRAF6. Lysates from these cells were immunoprecipitated with an anti-Myc antibody and immunoblotted with an anti-FLAG antibody.
(G) BMDMs generated from WT and *Peli1*$^{-/-}$ mice were in the presence or absence of M1 (IFN-γ + LPS) conditions for 3 hr. Cell lysates were harvested for immunoprecipitation with an anti-IRF5 antibody. These immunoprecipitated samples were immunoblotted for Pellino-1, IRF5, or TRAF6.
TCL, total cell lysate. See also Figure S1.

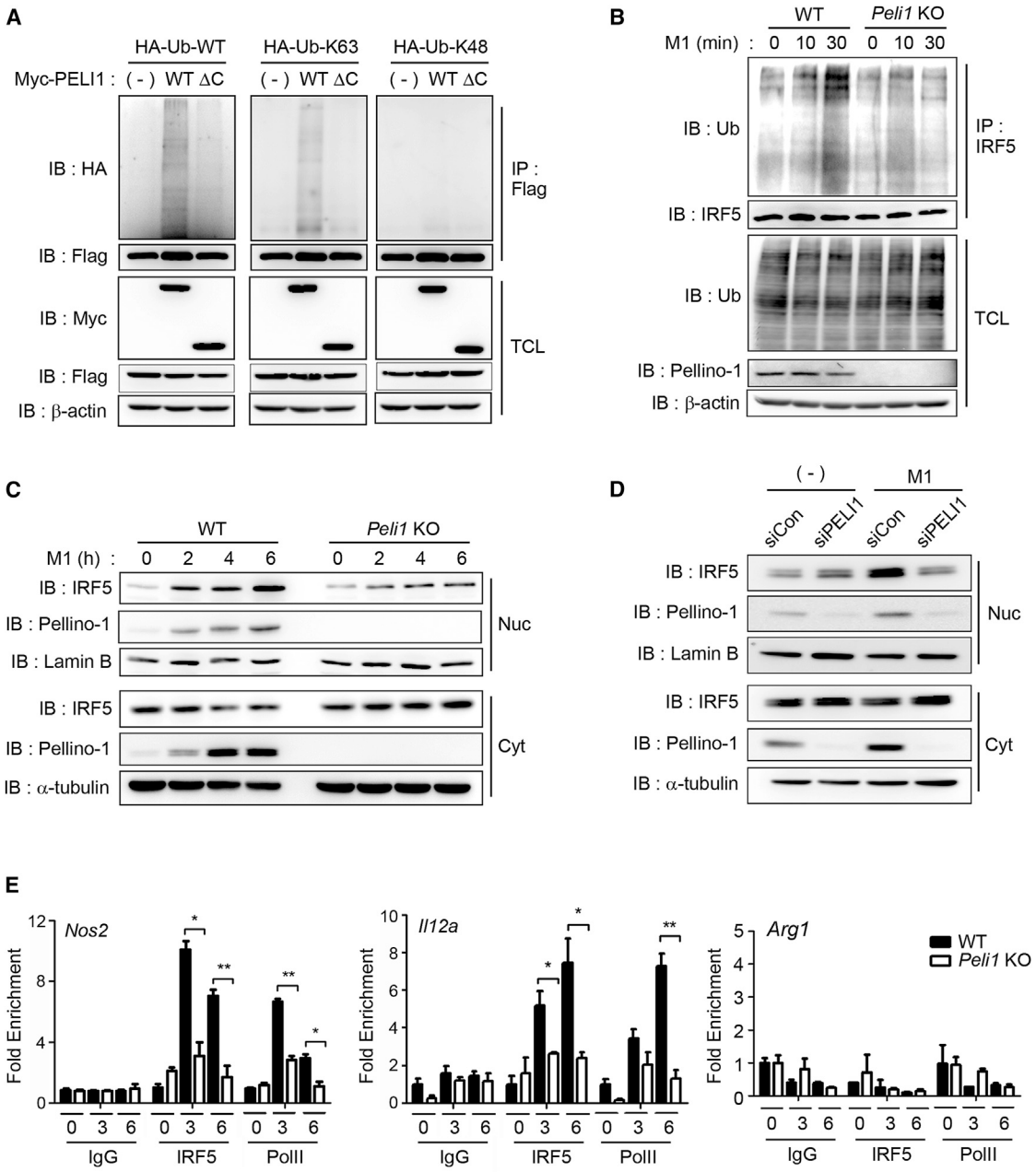

Figure 2. Pellino-1 Induces K63-Linked Ubiquitination of IRF5, Thereby Enhancing the Nuclear Translocation of IRF5 during M1 Macrophage Polarization

(A) 293T cells were co-transfected with FLAG-*IRF5* and the full-length (Myc-*PELI1*-WT) or C-terminal RING-domain deletion mutant (Myc-*PELI1*-ΔC) of Myc-*PELI1* in combination with HA-Ub (WT), K63-Ub, or K48-Ub expression plasmids. Cell lysates were harvested for immunoprecipitation with an anti-FLAG antibody and immunoblotted with an anti-HA antibody.

(B and C) BMDMs generated from WT or *Peli1*$^{-/-}$ mice were stimulated with IFN-γ + LPS. (B) The lysates of these cells were immunoprecipitated with an anti-IRF5 antibody and blotted with an anti-ubiquitin antibody. (C) The cytosolic and nuclear fractions were isolated from the lysates of these cells and immunoblotted for IRF5 or Pellino-1.

(D) The cytosolic and nuclear fractions were isolated from the lysates of HMDMs that had been transfected with a *PELI1* or control small interfering RNA (siRNA) and stimulated with IFN-γ + LPS; the fractions were blotted for IRF5 or Pellino-1.

(E) The lysates of BMDMs that had been simulated with IFN-γ + LPS were used for the chromatin immunoprecipitation (ChIP) assay using anti-IRF5, anti-RNA polymerase II, or control antibodies, and then the precipitated samples were used for real-time PCR for *Nos2*, *Il12a*, and *Arg1* promoters. IgG, immunoglobulin G. Data are presented as the mean ± SEM. *p < 0.05; **p < 0.01.

TCL, total cell lysate; Ub, ubiquitin. See also Figure S1.

in WT BMDMs compared to Pellino-1-deficient BMDMs in a dose-dependent manner (Figures 2E and S1E). In contrast, minimal IRF5 binding to the *Arg1* promoter was observed in WT and Pellino-1-deficient BMDMs. Taken together, these results indicate that Pellino-1 induces K63-linked ubiquitination of IRF5 by their direct interaction and, subsequently, enhances its nuclear translocation and transcription factor activity, resulting in M1 macrophage polarization.

Upon LPS and/or IFN-γ Stimulation, Pellino-1 Promotes M1 Polarization of Mouse BMDMs and Human-Monocyte-Derived Macrophages In Vitro

Considering Pellino-1-mediated K63-linked ubiquitination of IRF5 in M1 macrophages, we hypothesized that Pellino-1 might play a critical role in M1 macrophage polarization. To address this, we generated BMDMs from WT or *Peli1*$^{-/-}$ mice. Pellino-1-deficient bone marrow cells differentiated into macrophages similar to WT cells and were referred to as M0 BMDMs (Figure S2A). Consistently, the numbers of macrophages in various organs were similar between WT and *Peli1*$^{-/-}$ mice (Figures S2B and S2C), indicating that macrophage differentiation was intact in various organs of the *Peli1*$^{-/-}$ mice. Upon IFN-γ, lipopolysaccharide (LPS), M1 (LPS + IFN-γ), or M2 (IL-4 + IL-13) stimulation, the levels of the *Peli1* transcript were increased by LPS or LPS + IFN-γ at early time points but were not altered by IFN-γ alone or IL-4 + IL-13 (Figure 3A). Compared with *Peli1* transcription, IFN-γ and/or LPS, but not M2 stimuli, increased the levels of the Pellino-1 protein in BMDMs at different time points (Figures 3B and S2D). We next cultured peripheral blood monocytes obtained from healthy donors to generate HMDMs and study functions of Pellino-1 in human macrophages. Consistent with murine BMDMs, the expression levels of Pellino-1 in HMDMs were significantly increased upon treatment with M1 stimuli but not M2 stimuli (Figures 3C, 3D, and S2F). These findings indicate that signaling through both TLR4 and the IFN-γ receptor increases the expression levels of Pellino-1 in M1 macrophages of humans and mice, although the kinetics of Pellino-1 expression of M1 macrophages appear to be slightly different in two species. Moreover, Pellino-1 expression was increased in macrophages from the adipose tissue of WT mice fed a high-fat diet (HFD), which induces M1 macrophage polarization in adipose tissue, compared to mice fed a normal chow diet (NCD) (Figures 3E, 3F, and S2G). Regarding M1-M2 polarization, the expression levels of the transcripts for M1 markers were decreased in BMDMs generated from *Peli1*$^{-/-}$ mice following IFN-γ and/or LPS stimulation compared with the BMDMs from *Peli1*$^{+/-}$ or WT mice, whereas the M2 marker levels were similar in these groups upon M2 polarization (Figures 3G, 3H, and S2E). Consistently, Pellino-1 knockdown in HMDMs decreased M1 marker expression during M1 polarization (Figure 3I). However, the deficiency in M1 polarization of Pellino-1-deficient BMDMs was not due to different expression levels of TLR4 or IFN-γ receptors on Pellino-1-deficient BMDMs (Figure S2H). Furthermore, inhibition or knockdown of RIP1, a target protein of Pellino-1 for TLR4 signaling in macrophages (Chang et al., 2009), minimally affected M1 polarization of WT BMDMs (Figures S2I and S2J). Several studies have reported that M1 and M2 macrophage polarization requires aerobic glycolysis and fatty acid oxidation, respectively (Huang et al., 2014; Tannahill et al., 2013). We, therefore, compared the metabolic phenotypes of BMDMs from WT and *Peli1*$^{-/-}$ mice to test whether Pellino-1 deficiency might affect metabolic profiles in macrophages. Upon M1 stimulation with IFN-γ + LPS, the Pellino-1-deficient BMDMs showed a significant reduction in extracellular acidification rates (ECARs) compared with the WT BMDMs (Figures 4A and 4C). However, the ECARs and oxygen consumption rates (OCRs) were similar in M0 and M2 BMDMs from WT or *Peli1*$^{-/-}$ mice (Figures 4A–4D). In contrast to the ECAR results, there was little difference in the OCR in BMDMs from WT and *Peli1*$^{-/-}$ mice in the absence or presence of M1 polarization (Figures 4B and 4D). These findings indicate that Pellino-1-deficient M1 BMDMs exhibit decreased glycolysis compared with WT M1 BMDMs. Together, these results indicate that TLR4 ligand and/or IFN-γ increase Pellino-1 expression in M1 macrophages, which is required for M1 polarization of mouse BMDMs and HMDMs in vitro.

Pellino-1-Mediated M1 Macrophage Polarization Affects the Regulation of Glucose Intolerance In Vivo

We adoptively transferred Pellino-1-deficient (CD45.2^{+}) or WT (CD45.2^{+}) M0 BMDMs into WT mice (CD45.1^{+}) that were fed an HFD for 6 weeks and then depleted the macrophages by injecting clodronate to confirm the functional role of Pellino-1 in M1 polarization in vivo (Figure 5A). In general, clodronate-encapsulated liposomes have been considered as the most efficacious reagent for macrophage depletion in vivo (Van Rooijen and Sanders, 1996). Adoptive transfer of Pellino-1-deficient or WT M0 BMDMs led to similar restoration of macrophages in the adipose tissues of WT mice that were fed an HFD for 6 weeks and then depleted of macrophages (Figures S3A and S3C). It is well known that the microenvironment of the adipose tissue in obese mice favors M1 macrophage polarization (Castoldi et al., 2016), and the expression of CD11c is indicative of M1 macrophage polarization, particularly in adipose tissue (Lumeng et al., 2007; Torres-Castro et al., 2016). Thus, we analyzed the CD11c expression pattern in transferred M0 BMDMs in adipose tissue to estimate how many transferred M0 BMDMs had differentiated into M1 macrophages. Approximately 35%–40% of the transferred WT M0 BMDMs expressed CD11c in the adipose tissue of WT mice fed an HFD, whereas 20%–25% of the transferred Pellino-1-deficient M0 BMDMs expressed CD11c (Figure 5B). In contrast, few of the transferred WT and Pellino-1-deficient M0 BMDMs were polarized into M2-type macrophages (Figures 5B and S3B). These findings indicate that fewer of the transferred Pellino-1-deficient M0 BMDMs differentiated into M1 macrophages in the adipose tissues of mice fed an HFD than WT M0 BMDMs (Figure 5B). However, adoptive transfer of WT or Pellino-1-deficient M0 BMDMs did not affect the M1 and M2 macrophage percentages of the recipient mice (Figure 5B) or the composition of other immune cells in the adipose tissues (Figure S3D). Consistently, the expression levels of M1 markers such as *Nos2* and *Il12a* were significantly increased in the stromal-vascular fraction (SVF) from WT mice fed an HFD for 8 weeks, depleted of macrophages, and adoptively transferred with WT BMDMs compared with Pellino-1-deficient BMDMs, whereas the M2 markers were similar in the two groups

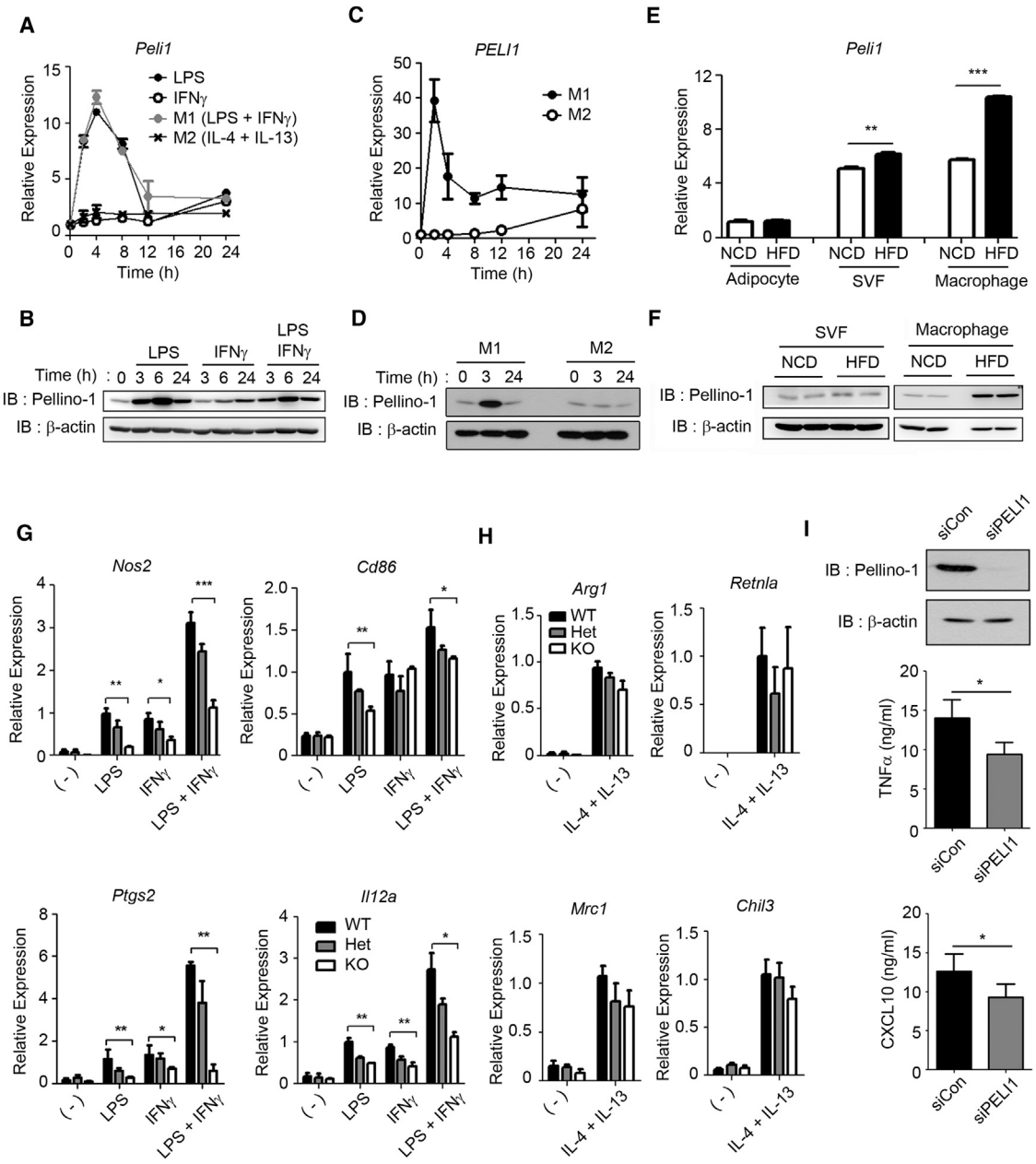

Figure 3. Pellino-1 Deficiency in Human and Mouse Macrophages Attenuates M1 Polarization In Vitro

(A and B) Pellino-1 expression in bone-marrow-derived macrophages (BMDMs) from wild-type (WT) mice upon stimulation with IFN-γ and/or LPS, or IL-4 + IL-13 using qRT-PCR (A) and immunoblotting (B).

(C and D) Peripheral blood mononuclear cells (PBMCs) were obtained from healthy donors and cultured with recombinant macrophage colony stimulating factor (M-CSF) for 7 days to generate human-monocyte-derived macrophages (HMDMs). Upon stimulation with IFN-γ + LPS or IL-4 + IL-13, the expression levels of *PELI1* and Pellino-1 in HMDMs were measured using qRT-PCR (C) and immunoblotting (D), respectively, at the indicated time points.

(E and F) Adipocytes, stromal-vascular fraction (SVF) cells, and F4/80^{+} macrophages were obtained from WT mice that were fed a high-fat diet (HFD) or normal chow diet (NCD) for 8 weeks, and Pellino-1 expression was estimated using qRT-PCR (E) and immunoblotting (F).

(G and H) BMDMs generated from WT, *Peli1*$^{+/-}$ (Het), or *Peli1*$^{-/-}$ (KO) mice were stimulated with IFN-γ and/or LPS (G) or IL-4 + IL-13 (H) for 24 hr, and the expression of various M1 or M2 markers in macrophages was estimated.

(I) The expression levels of M1 markers in HMDMs that were transfected with siRNA for *PELI1* or control and treated with IFN-γ + LPS were estimated.

Data are presented as the mean ± SEM.*p < 0.05; **p < 0.01; ***p < 0.001.

See also Figure S2.

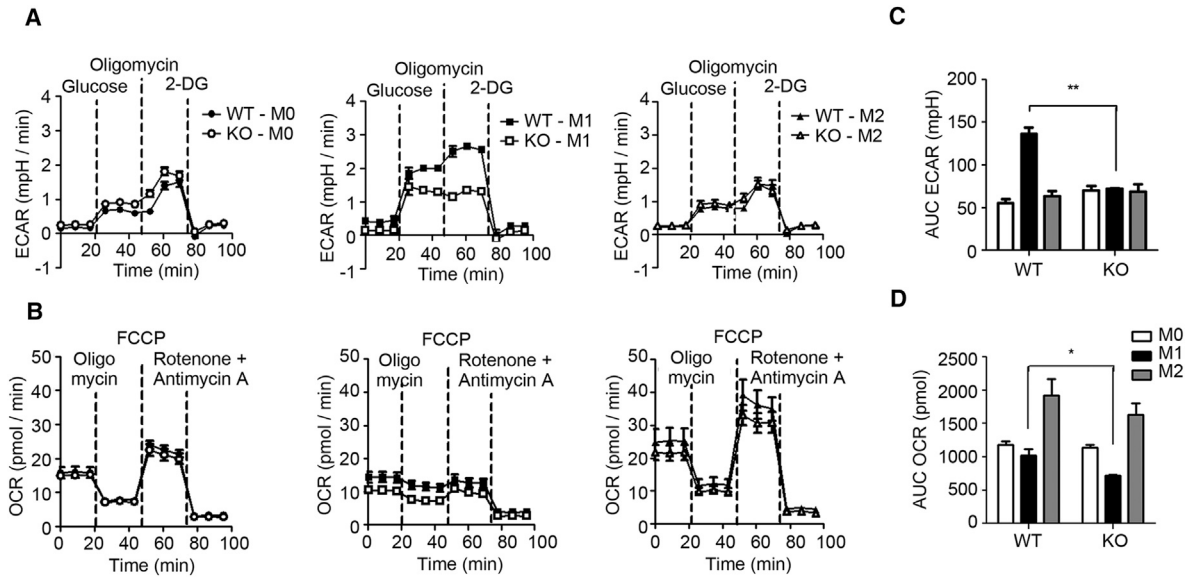

Figure 4. Pellino-1 Deficiency Reduces Glycolysis in BMDMs during M1 Polarization

(A and B) WT and Pellino-1-deficient BMDMs were unstimulated (left) or stimulated with LPS + IFN-γ (middle) or IL-4 + IL-13 (right) for 6 hr, and the extracellular acidification rates (ECARs) (A) and oxygen consumption rates (OCRs) (B) were measured. For the ECAR measurement, BMDMs were sequentially treated with glucose (10 mM), oligomycin (1 μM), and 2-DG (50 mM), whereas oligomycin (1 μM), FCCP (1 μM), rotenone (1 μM), and antimycin A (1 μM) were added to BMDMs to estimate OCR.

(C and D) Areas under the curve (AUCs) for ECAR (C) and OCR (D) in the WT and Pellino-1-deficient BMDMs were calculated and compared.

Data are presented as the mean ± SEM. *$p < 0.05$; **$p < 0.01$.

(Figure 5C). Collectively, these results indicate that Pellino-1 promotes M1 macrophage polarization in vivo.

Next, we performed the glucose tolerance test (GTT) and insulin resistance test (ITT) in these mice to explore whether Pellino-1-mediated M1 macrophage polarization in the adipose tissues affects glucose tolerance in vivo. Glucose levels in the GTT and ITT were increased in mice in which WT M0 BMDMs were adoptively transferred, compared to mice that were adoptively transferred with Pellino-1-deficient M0 BMDMs (Figures 5D and 5E). Upon insulin stimulation, the expression levels of phosphorylated AKT (p-AKT) and phosphorylated ERK (p-ERK) were increased in mice that were adoptively transferred with Pellino-1-deficient BMDMs, compared to mice given WT BMDMs (Figure 5F). Consistent with these findings, *Peli1*$^{+/-}$ littermates showed higher glucose levels in the GTT and ITT than *Peli1*$^{-/-}$ mice after being fed an HFD (Figures 6A and 6B). Consistently, the homeostatic model assessment-insulin resistance (HOMA-IR) indexes, M1/M2 macrophage ratios and M1 marker expression levels in SVF cells, and crown-like structures in adipose tissues were increased, whereas insulin-induced expression levels of p-AKT and p-ERK were decreased in *Peli1*$^{+/-}$ littermates compared with *Peli1*$^{-/-}$ mice after being fed an HFD (Figures 6C–6G and S3E). Among T cell-mediated cytokines, the transcript levels of *Il17a* were significantly lower in the SVF of *Peli1*$^{-/-}$ mice than in that of *Peli1*$^{+/-}$ littermates, suggesting that the Pellino-1-IRF5 axis in M1 macrophages may affect CD4^{+} T cell polarization in adipose tissues (Figure S3F). The body and fat weights were reduced in *Peli1*$^{-/-}$ mice compared with *Peli1*$^{+/-}$ mice after being fed an HFD, but not an NCD, although food intake in the two groups was similar (Figures 6H–6J). Consistently, these parameters in *Peli1*$^{+/+}$ mice were significantly different from those in *Peli1*$^{-/-}$ mice (Figures S4A–S4J) but similar to those in *Peli1*$^{+/-}$ littermates (Figures S5A–S5H). Together, these results indicate that Pellino-1-mediated M1 macrophage polarization contributes to the regulation of glucose intolerance in vivo.

Human Macrophages Enhance Pellino-1 Expression and the Nuclear Translocation of IRF5 upon M1 Polarization in Adipose Tissues of Obese Humans

We collected peritoneal adipose tissues from volunteer patients who underwent laparoscopic gastrectomy for early gastric cancer to validate Pellino-1-mediated M1 macrophage polarization in the adipose tissue of obese humans (Table S1). The subject's body mass index (BMI) was significantly associated with their waist circumference, HOMA-IR, the total percentages of CD14^{+} cells among CD45^{+} immune cells, and the percentages of M1 macrophages among CD14^{+} cells from the adipose tissue, although no association was found for the M2 macrophage percentages (Figures S6A and S6B). The expression levels of the *PELI1* and *IRF5* transcripts in CD14^{+} cells from adipose tissue were higher in obese subjects than in non-obese subjects and significantly associated each other (Figures 7A, 7B, S6C, and S6D). *PELI1* expression was also significantly associated with the HOMA-IR and percentages of M1 macrophages among CD14^{+} cells in adipose tissue (Figures 7C–7E), and there was a tendency for *PELI1* expression to be correlated with the BMI, although the correlation was not significant (Figure S6D). However, there was no difference in Pellino-1 expression in obese non-diabetic versus obese diabetic patients (Figure S6E), and

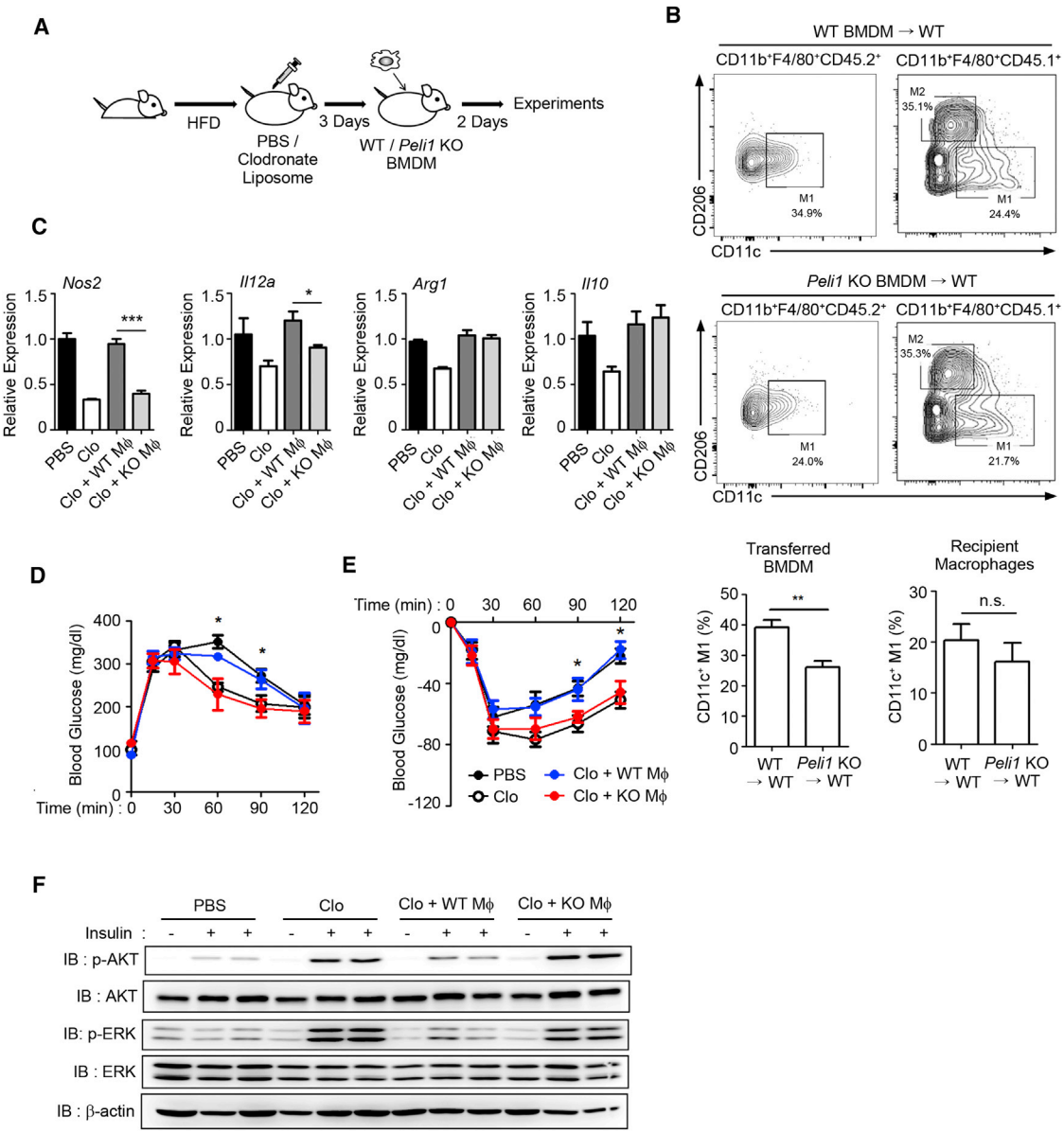

Figure 5. Pellino-1-Deficient BMDMs Attenuate M1 Polarization In Vivo, which Contributes to the Regulation of Glucose Metabolism in Mice Fed an HFD

(A) Diagram of the experimental scheme for the adoptive transfer of M0 BMDMs into WT mice fed an HFD.

(B) SVF cells were obtained from the adipose tissues of WT mice (CD45.1$^+$) that were fed an HFD for 6 weeks, depleted of macrophages using clodronate, and adoptively transferred with M0 BMDMs generated from WT (CD45.2$^+$) or *Peli1*$^{-/-}$ (CD45.2$^+$) mice as described in (A). These SVF cells were analyzed for the percentages of donor and recipient macrophages by examining CD45.1 (donor) versus CD45.2 (recipient) expression. The percentages of M1 or M2 macrophages were determined in terms of the expression patterns of CD11c versus CD206 among the CD11b$^+$F4/80$^+$ macrophages.

(C–F) WT mice were fed an HFD for 6 weeks, injected with PBS liposomes or clodronate liposomes, and then adoptively transferred with Pellino-1-deficient or WT M0 BMDMs (n = 6 per group). (C) The expression levels of M1 and M2 markers were estimated in SVF cells from the visceral adipose tissues. (D) The glucose tolerance test (GTT) and (E) insulin tolerant test (ITT) were performed. Blood glucose levels were determined at the indicated time points after an intraperitoneal injection of glucose (1.5 g/kg) or insulin (0.75 U/kg). (F) Immunoblotting for AKT, phosphorylated AKT (p-AKT), ERK, and p-ERK was performed using lysates of the visceral adipose tissues obtained from mice that were intraperitoneally administered PBS or insulin (1 U/kg) 10 min before euthanasia.

Data are presented as the mean ± SEM. *p < 0.05; **p < 0.01; ***p < 0.001; n.s., not significant.

See also Figure S3.

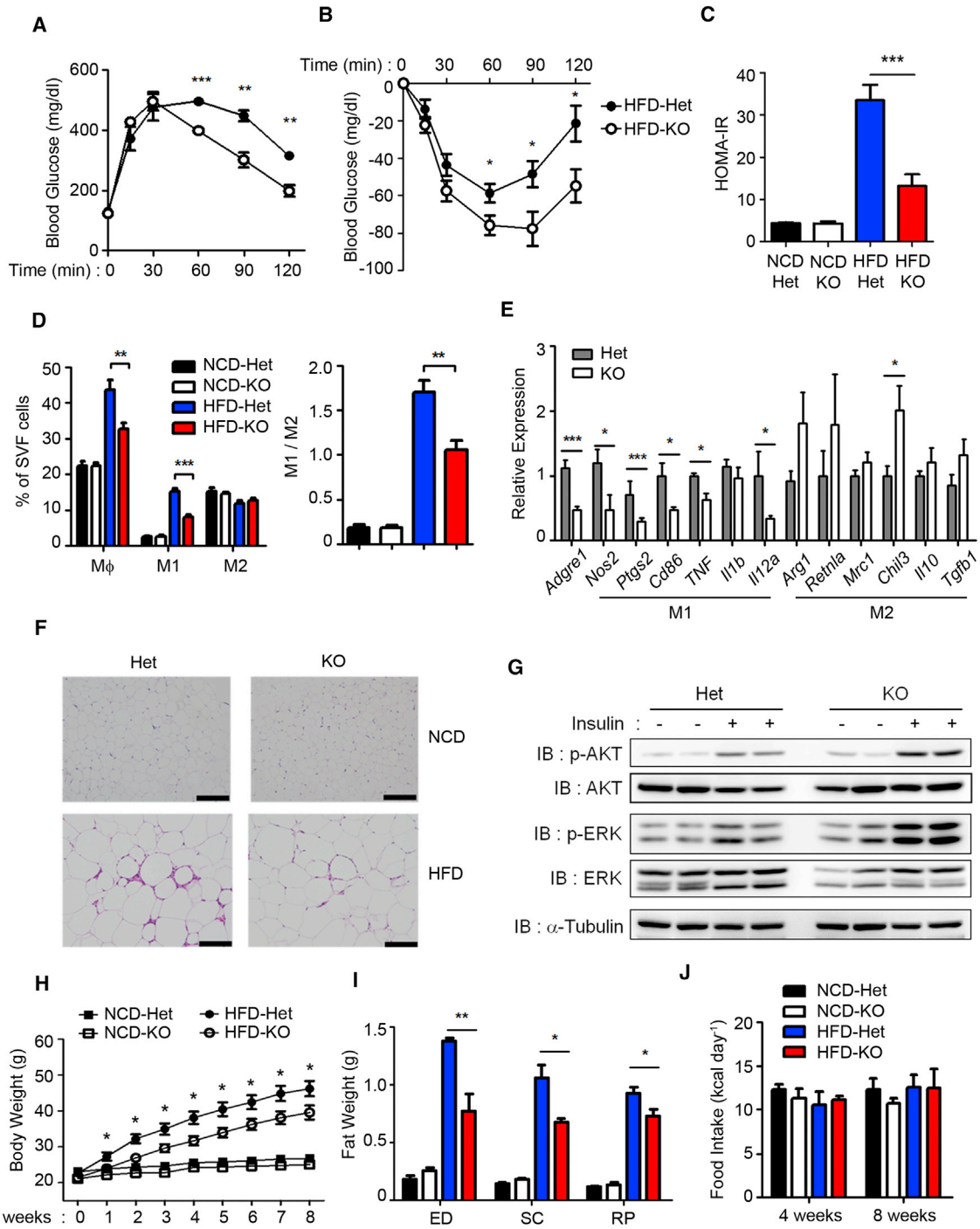

Figure 6. Pellino-1 Deficiency Attenuates Obesity-Induced Glucose Intolerance

(A–J) Male *Peli1*$^{-/-}$ (KO) and *Peli1*$^{+/-}$ (Het) littermates were fed an NCD or HFD for 8 weeks.

(A) The blood glucose levels in *Peli1*$^{-/-}$ mice (n = 5) and *Peli1*$^{+/-}$ littermates (n = 5) were determined at the indicated time points after fasting overnight and an intraperitoneal injection of glucose (1.5 g/kg).

(B) The blood glucose levels in *Peli1*$^{-/-}$ mice (n = 5) and *Peli1*$^{+/-}$ littermates (n = 5) were measured at the indicated time points after fasting for 4 hr and an intraperitoneal injection of insulin (0.75 U/kg).

(C) HOMAR-IR was determined in *Peli1*$^{-/-}$ mice and *Peli1*$^{+/-}$ littermates (n = 10 per group).

(D) The percentages of CD11b^{+}F4/80^{+} macrophages, CD11c^{+}CD11b^{+}F4/80^{+} M1 macrophages, and CD206^{+}CD11b^{+}F4/80^{+} M2 macrophages among the SVF cells were determined in the visceral adipose tissues from *Peli1*$^{-/-}$ mice (n = 6) and *Peli1*$^{+/-}$ littermates (n = 6).

(legend continued on next page)

PELI1 expression was not significantly associated with *TGFB1* expression (Figure S6D), which has been reported to be regulated by IRF5 in human adipose tissue macrophages (Dalmas et al., 2015). Furthermore, $CD14^+$ cells from obese humans showed higher Pellino-1 expression in the cytosolic fraction and nuclear translocation of IRF5 than cells from lean humans (Figure 7F), which was also observed in the immunohistochemistry of adipose tissues (Figure 7G). Moreover, crown-like structures were frequently observed in the adipose tissues from obese subjects compared with those from non-obese subjects. Together, these findings indicate that Pellino-1 expression is increased in human macrophages from obese adipose tissue, which promotes M1 polarization and IRF5 nuclear translocation.

DISCUSSION

Chang et al. reported that Pellino-1 activated nuclear factor κB (NF-κB) in macrophages by RIP1 ubiquitination upon TLR4-mediated stimulation (Chang et al., 2009), suggesting that Pellino-1 expression might promote M1 polarization by inducing RIP1 ubiquitination. However, this mechanism appears to be less likely, because inhibition or knockdown of RIP1 in BMDMs minimally affected M1 polarization. Instead, we showed that Pellino-1 induced K63-linked ubiquitination of IRF5 via direct interaction and enhanced nuclear translocation of IRF5 during M1 macrophage polarization (Figures 1 and 2). Based on these findings, it is feasible that, upon TLR4 engagement, Pellino-1 might exert dual functions in macrophages by providing RIP1-mediated NF-κB activation as a TLR4 downstream signal component and promoting IRF5-dependent M1 polarization as a common mediator of TLR4 and IFN-γ receptor. The cytosolic and nuclear expressions of Pellino-1 in BMDMs were increased upon M1 polarization stimulation, suggesting that both cytosolic and nuclear Pellino-1 might play functional roles in M1 macrophage polarization. However, the IRF5-Pellino-1 interaction was found in the cytosolic, but not the nuclear, fraction of 293T cells and increased nuclear translocation of IRF5 during M1 polarization, indicating that cytosolic Pellino-1 binds to IRF5 and induces its ubiquitination in the cytosolic compartment before IRF5 translocates into the nuclear compartment. Collectively, it is most likely that cytosolic Pellino-1 significantly contributes to IRF5 ubiquitination and activation during M1 polarization, although the functional role of nuclear Pellino-1 remains elusive. Consistently, it was reported that IRF5 contributed to M1 macrophage polarization by directly activating the transcription of IL-12 subunits in mice (Krausgruber et al., 2011), which was consistent with the reduced levels of IL-12 in Pellino-1-deficient macrophages compared with WT macrophages in vitro and in vivo (Figures 3G and 5C). Upon TLR7 engagement, the activation and nuclear translocation of IRF5 are induced by IKKβ-mediated phosphorylation at Ser 462 or TRAF6-mediated K63-linked ubiquitination of lysine residues at positions 410 and 411, thereby promoting IRF5-mediated pro-inflammatory cytokine production (Balkhi et al., 2008; Ren et al., 2014), which might account for residual nuclear translocation of IRF5 in Pellino-1-deficient BMDMs. However, the IRF5-Pellino-1 interaction, but not the IRF5-TRAF6 interaction, was increased in M1-polarized BMDMs (Figure 1G), indicating that TRAF6-mediated, K63-linked IRF5 ubiquitination minimally occurs during M1 macrophage polarization. Moreover, a chromatin immunoprecipitation assay revealed that IRF5 binding to the *Il12a* and *Nos2* promoters was reduced in Pellino-1-deficient BMDMs. These findings suggest that cytosolic Pellino-1-mediated, K63-linked ubiquitination of IRF5 might play a critical role in M1 macrophage polarization. Furthermore, Pellino-1 expression was increased in macrophages upon TLR4 ligand and/or IFN-γ stimulation, and Pellino-1-deficient BMDMs were defective in M1 polarization induced by LPS and/or IFN-γ in vitro and an HFD in vivo, suggesting that Pellino-1 promotes M1 macrophage polarization as a common functional regulator to integrate signals through TLR4 and/or IFN-γ receptor. Meanwhile, it has been reported that IRF4 competes with IRF5 and acts as a negative regulator of TLR signaling (Negishi et al., 2005). However, it is not likely that Pellino-1 might interact with IRF4 during M1 macrophage polarization, because IRF4 is minimally detected in M1 macrophages (data not shown). Together, these findings suggest that IRF5-Pellino-1 interaction in the cytoplasm promotes M1 macrophage polarization by linking TLR4 and/or IFN-γ receptor and IRF5 in M1 macrophages.

Pellino-1-mediated M1 macrophage polarization is consistent with the Pellino-1-mediated pro-inflammatory function of microglia via TRAF3 (Xiao et al., 2013). These combined results suggest that macrophages in the CNS and adipose tissue are classically activated by Pellino-1 but require different target proteins. In contrast to Pellino-1, Pellino-3 attenuated M1 macrophage polarization by inhibiting TRAF6-mediated ubiquitination of HIF-1α (Yang et al., 2014). These findings suggest that Pellino-1 and Pellino-3 inversely regulate M1 macrophage polarization. Macrophages exhibit a distinct metabolic profile during M1 and M2 polarization (O'Neill and Pearce, 2016); M1 macrophages shift toward anaerobic glycolysis, whereas M2 macrophages use oxidative phosphorylation to generate ATP (Galván-Peña and O'Neill, 2014; Huang et al., 2014). Consistent with these observations, Pellino-1-deficient BMDMs showed

(E) The expression levels of M1 and M2 markers were estimated in the SVF cells from the visceral adipose tissues of *Peli1*$^{-/-}$ (n = 8) mice and *Peli1*$^{+/-}$ littermates (n = 8).
(F) The microscopic examination was performed using visceral adipose tissues (H&E staining) from *Peli1*$^{-/-}$ and *Peli1*$^{+/-}$ mice. Scale bars represent 50 μm.
(G) The visceral adipose tissues were obtained frosm *Peli1*$^{-/-}$ and *Peli1*$^{+/-}$ littermates that had been intraperitoneally injected with PBS or insulin (1 U/kg) after being fed an HFD for 8 weeks and fasted overnight. Immunoblotting for AKT, p-AKT, ERK, and p-ERK was performed using these adipose tissues.
(H and I) (H) Body and (I) fat (ED, epididymal; SC, subcutaneous; and RP, retroperitoneal) weights were measured in mice that were fed an NCD (n = 12 per group) or HFD (n = 15 per group).
(J) The amount of food intake (NCD and HFD) by *Peli1*$^{-/-}$ (n = 8) and *Peli1*$^{+/-}$ littermates (n = 8) was estimated.
Data are presented as the mean ± SEM. *p < 0.05; **p < 0.01; ***p < 0.001.
See also Figures S3–S5.

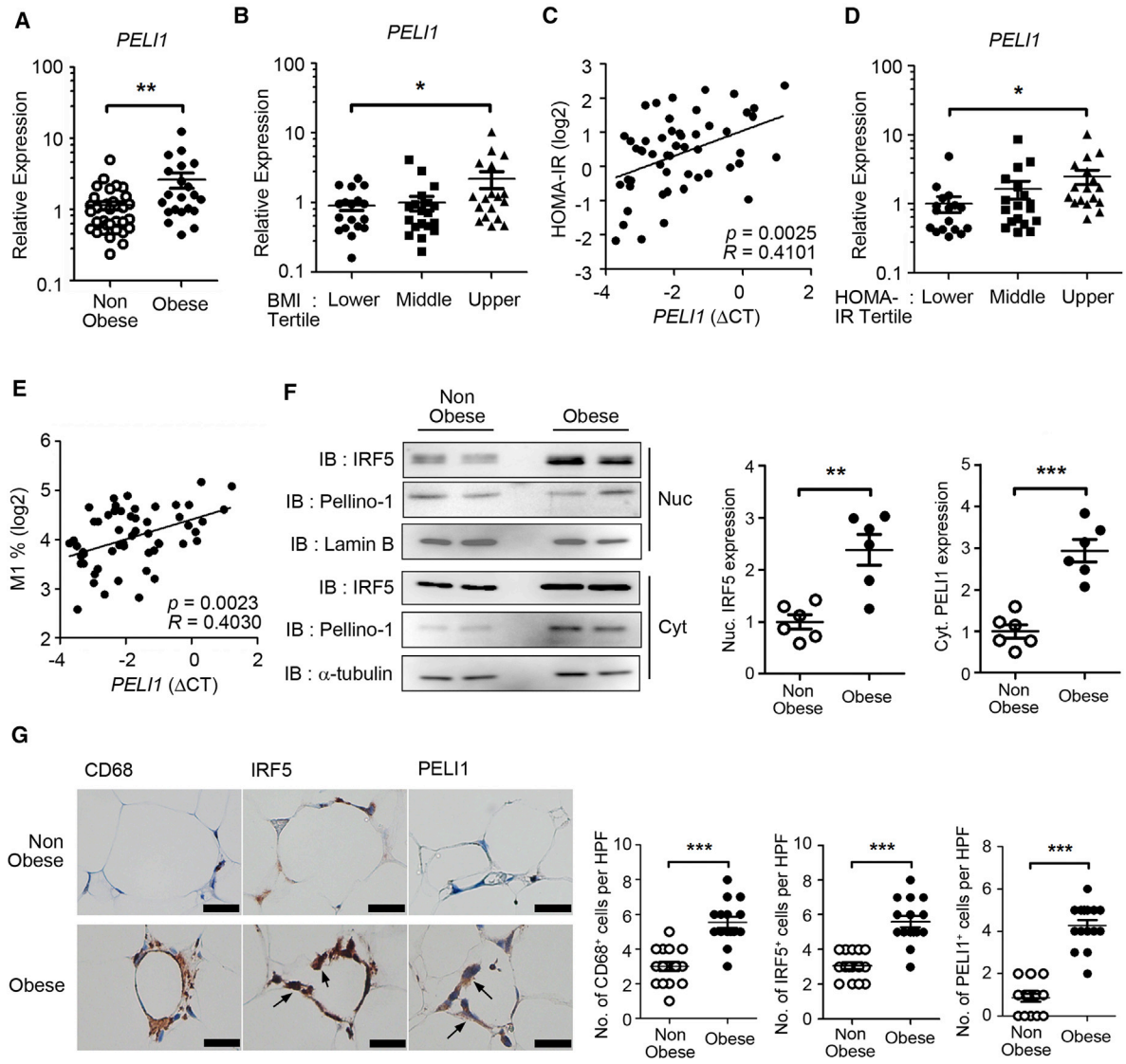

Figure 7. Human Macrophages Exhibit Increased Pellino-1 Expression and Nuclear Translocation of IRF5 in Obese Adipose Tissues Compared with Non-obese Adipose Tissues

(A–E) $CD14^+$ cells were isolated from the visceral fat tissues of obese (n = 21) and non-obese (n = 34) humans. (A) The expression levels of the *PELI1* transcript were measured in these $CD14^+$ cells from obese versus non-obese humans and compared according to (B) the tertiles of body mass index (BMI) (tertiles: lower, 18–23.1; middle, 23.3–25.4; upper, 25.5–35.6), (C and D) HOMA-IR (tertiles: lower, 0.2–1.0; middle, 1.1–2.0; upper, 2.1–5.2), and (E) percentages of M1 macrophages among $CD14^+$ cells. To analyze data based on tertiles, patients were divided into three parts based on an ordered distribution of BMI or HOMA-IR (B and D, respectively).

(F) The cytosolic and nuclear fractions isolated from these $CD14^+$ cell lysates were immunoblotted for IRF5 or Pellino-1. $CD14^+$ cells in the adipose tissues of non-obese or obese humans were collected for each sample and used for immunoblotting (left), which were analyzed and presented in graphs (right).

(G) Immunohistochemistry was performed for CD68, Pellino-1, and IRF5 using the visceral adipose tissues obtained from obese and non-obese humans (left), which were analyzed and presented in graphs (right). Scale bars represent 20 μm.

*p < 0.05; **p < 0.01; ***p < 0.001. In (C) and (E), the correlation analysis was performed using the non-parametric Spearman's test. In (F) and (G), data are representative of three independent experiments.

See also Figure S6.

less glycolysis than WT BMDMs upon M1 polarization, suggesting that Pellino-1 is involved in regulating glycolysis during M1 polarization. Although the mechanisms by which Pellino-1 regulates glycolysis in M1 macrophages are unclear, it is hypothesized that Pellino-1 might regulate glycolysis directly by inducing the ubiquitination of target proteins in the glycolysis pathway, indirectly through promoting M1 polarization itself, or both.

Based on the critical role of Pellino-1-IRF5 interaction in M1 polarization, we postulated that Pellino-1 might be involved in

regulating M1-macrophage-dependent diseases (Chawla et al., 2011; Lawrence and Natoli, 2011; Sica and Bronte, 2007; Sica and Mantovani, 2012). Among these diseases, our experiments showed that Pellino-1 regulated glucose intolerance by promoting M1 macrophage polarization via IRF5 ubiquitination in mice fed an HFD and in obese humans. Moreover, increased insulin-induced expression levels of p-AKT and p-ERK in the adipose tissue of Pellino-1-deficient mice or WT mice that were given Pellino-1-deficient macrophages and fed an HFD, as well as a positive correlation between HOMA-IR and Pellino-1 expression in $CD14^+$ cells from the adipose tissue of obese humans, suggest that Pellino-1 expression in M1 macrophages might contribute to regulating obesity-induced insulin resistance in mice and humans. IRF5 is known to be implicated in several diseases, including systemic lupus erythematosus and diet-induced insulin resistance (Dalmas et al., 2015; Graham et al., 2007; Saigusa et al., 2015; Weiss et al., 2015). Furthermore, IRF5-deficient mice exhibited increased accumulation of M2 macrophages, collagen deposition in adipose tissues, and insulin sensitivity, suggesting that IRF5 is involved in obesity-induced insulin resistance by regulating macrophages and adipocytes (Dalmas et al., 2015). However, IRF5 transcripts were detected at minimal levels in human adipocytes but were highly expressed in $CD14^+$ monocytes (Dalmas et al., 2015). Moreover, Pellino-1 was also minimally expressed in adipocytes in mice fed an NCD or HFD (data not shown). Thus, it is more likely that the direct interaction between Pellino-1 and IRF5 occurs in M1-polarized macrophages rather than in adipocytes during obesity-induced insulin resistance. Consistent with this result, the macrophages in adipose tissues from obese humans and mice showed increased nuclear translocation of IRF5, compared with the non-obese controls, which was attenuated by Pellino-1 knockdown or knockout. However, there is a discrepancy in phenotypes of Pellino-1 knockout (KO) and myeloid-specific IRF5 KO mice in the HFD model (Dalmas et al., 2015), which might be attributable to the Pellino-1 expression pattern in various immune and non-immune cells and Pellino-1-independent IRF5 activation (Balkhi et al., 2008; Chang et al., 2009, 2011; Ordureau et al., 2008; Ren et al., 2014). Collectively, these results show that the Pellino-1-IRF5 axis in M1-polarized macrophages may represent a pathway to regulate glucose metabolism in vivo.

In conclusion, our experiments show that Pellino-1-IRF5 interaction in human and mouse macrophages induces K63-linked ubiquitination of IRF5, thereby establishing the TLR4/IFN-γR-Pellino-1-IRF5 axis in M1 macrophage polarization and regulating glucose intolerance in obesity.

EXPERIMENTAL PROCEDURES

Human Study Population

Individuals scheduled to undergo laparoscopic gastrectomy for early gastric cancer at Seoul National University Hospital, Seoul, Korea, from December 2015 through December 2016 were included in this study. This study followed the recommendations of the World Medical Association and the Declaration of Helsinki. Thus, each participant signed written informed consent, and this study was approved by the Institutional Review Board of Seoul National University Hospital (H-1510-036-710). For details, see the Supplemental Experimental Procedures.

Mice and In Vivo Experiments

Peli1$^{+/-}$ mice (C57BL/6 × 129/Sv background) were generated as previously described (Jeon et al., 2011) (Figure S7) and backcrossed onto the C57BL/6 background for at least seven generations to generate the *Peli1*$^{-/-}$ mice. All experiments were approved by the Institutional Animal Care and Use Committee in Seoul National University Hospital (SNUH-IACUC), and animals were maintained in the AAALAC-International-accredited facility (#001169). Age- and sex-matched littermate mice were used for all experiments. Eight-week-old littermate *Peli1*$^{+/-}$ and *Peli1*$^{-/-}$ mice were fed an HFD (D12492, Research Diets) for the indicated duration to induce the HFD model. Details are included in the Supplemental Experimental Procedures.

Preparation of Bone-Marrow- or Monocyte-Derived Macrophages from Mice and Humans

The mouse BMDMs, prepared from the femurs and tibias of 8- to 12-week-old mice, were flushed with sterile 1 × PBS, and red blood cells were lysed with RBC Lysis Solution (QIAGEN). Peripheral blood samples were collected from healthy volunteers after obtaining informed consents at Seoul National University College of Medicine (Institutional Review Board [IRB] No. 1306-002-491) to prepare HMDMs. Details are included in the Supplemental Experimental Procedures.

ECAR and OCR Measurements

Approximately 2 × 10^5 BMDMs were plated in XF24 cell-culture microplates (Seahorse Bioscience) and treated with M1 or M2 stimuli for the indicated times to analyze the ECAR and OCR. After stimulation, the media were changed to XF assay media, according to the manufacturer's instructions. The ECAR and OCR were assessed using an XF24 analyzer (Seahorse Bioscience). These data were normalized to the total protein contents, which were measured using a Bradford protein assay (Bio-Rad).

qRT-PCR

Total RNAs, which were isolated from cells using TRIzol (Life Technologies), were reverse transcribed into cDNAs using RNA M-MLV reverse transcriptase (Promega) according to the manufacturer's protocol. Gene-specific PCR products were measured using an Applied Biosystems 7500 Sequence Detection System (Perkin-Elmer Biosystems). Details are included in the Supplemental Experimental Procedures.

Immunoprecipitation and Immunoblotting

For immunoprecipitations, the cell lysates were prepared from BMDMs or 293T cells transiently transfected with expression vectors, using the conventional calcium-mediated transfection method and used for immunoprecipitation. The eluted samples were loaded onto 8% SDS-PAGE gels and transferred onto a polyvinylidene fluoride membrane (Millipore) for western blotting. For details, see the Supplemental Experimental Procedures.

Chromatin Immunoprecipitation

The Pierce Agarose ChIP Kit (Thermo Fisher) was used according to the manufacturer's protocols. For details, see the Supplemental Experimental Procedures.

Flow Cytometry

Human and mouse SVF cells were isolated as previously described (Huh et al., 2013) and used for flow cytometry or RNA extraction. Single-cell suspensions were pre-incubated with mouse or human anti-Fc receptor antibodies (BD Biosciences), stained for 30 min at 4°C, washed twice, and analyzed by flow cytometry with a BD LSR II machine.

Statistical Analysis

All experiments were repeated at least three times. The data were presented as the mean ± SEM. Student's t tests (two groups) and one-way ANOVA (more than two groups) with Tukey's post hoc test were performed to compare the groups. The non-parametric Spearman's test was performed for the correlation analysis. All data were statistically

analyzed using GraphPad Prism 5 software. p values < 0.05 were considered significant.

SUPPLEMENTAL INFORMATION

Supplemental Information includes Supplemental Experimental Procedures, seven figures and one table and can be found with this article online at http://dx.doi.org/10.1016/j.celrep.2017.06.088.

AUTHOR CONTRIBUTIONS

D.K. performed the majority of in vitro and in vivo experiments, with contribution from J.K. and J.S.K. H.L. generated *Peli1* KO mice. Y.K.J. contributed to histological analysis. B.R.Y. and W.-W.L. performed and analyzed in vitro experiments using human macrophages. T.H.K., Y.-S.S., H.-J.L., and H.-K.Y. provided human visceral fat tissues from patients. C.W.L. provided reagents. H.Y.K., Y.M.C., and K.S.P. contributed to analyzing and interpreting data. D.H.C. designed and supervised the study and wrote the manuscript.

ACKNOWLEDGMENTS

This research was supported by a grant from the Korea Health Technology R&D Project through the Korea Health Industry Development Institute (KHIDI), funded by the Ministry of Health & Welfare, Republic of Korea (grant number: HI14C1277), and a grant from the National R&D Program for Cancer Control, Ministry for Health and Welfare, Republic of Korea (1220220). D.K. received a scholarship from the BK21-plus education program provided by the National Research Foundation of Korea. We would like to thank the Hyehwa Forum members for their helpful discussions and the NIH Tetramer Core Facility for providing CD1d tetramers.

Received: September 23, 2016
Revised: May 9, 2017
Accepted: June 28, 2017
Published: July 25, 2017

REFERENCES

Balkhi, M.Y., Fitzgerald, K.A., and Pitha, P.M. (2008). Functional regulation of MyD88-activated interferon regulatory factor 5 by K63-linked polyubiquitination. Mol. Cell. Biol. *28*, 7296–7308.

Castoldi, A., Naffah de Souza, C., Câmara, N.O., and Moraes-Vieira, P.M. (2016). The macrophage switch in obesity development. Front. Immunol. *6*, 637.

Chang, M., Jin, W., and Sun, S.C. (2009). Peli1 facilitates TRIF-dependent Toll-like receptor signaling and proinflammatory cytokine production. Nat. Immunol. *10*, 1089–1095.

Chang, M., Jin, W., Chang, J.H., Xiao, Y., Brittain, G.C., Yu, J., Zhou, X., Wang, Y.H., Cheng, X., Li, P., et al. (2011). The ubiquitin ligase Peli1 negatively regulates T cell activation and prevents autoimmunity. Nat. Immunol. *12*, 1002–1009.

Chawla, A., Nguyen, K.D., and Goh, Y.P. (2011). Macrophage-mediated inflammation in metabolic disease. Nat. Rev. Immunol. *11*, 738–749.

Dalmas, E., Toubal, A., Alzaid, F., Blazek, K., Eames, H.L., Lebozec, K., Pini, M., Hainault, I., Montastier, E., Denis, R.G., et al. (2015). Irf5 deficiency in macrophages promotes beneficial adipose tissue expansion and insulin sensitivity during obesity. Nat. Med. *21*, 610–618.

Galván-Peña, S., and O'Neill, L.A. (2014). Metabolic reprograming in macrophage polarization. Front. Immunol. *5*, 420.

Graham, R.R., Kyogoku, C., Sigurdsson, S., Vlasova, I.A., Davies, L.R., Baechler, E.C., Plenge, R.M., Koeuth, T., Ortmann, W.A., Hom, G., et al. (2007). Three functional variants of IFN regulatory factor 5 (IRF5) define risk and protective haplotypes for human lupus. Proc. Natl. Acad. Sci. USA *104*, 6758–6763.

Grosshans, J., Schnorrer, F., and Nüsslein-Volhard, C. (1999). Oligomerisation of Tube and Pelle leads to nuclear localisation of Dorsal. Mech. Dev. *81*, 127–138.

Huang, S.C., Everts, B., Ivanova, Y., O'Sullivan, D., Nascimento, M., Smith, A.M., Beatty, W., Love-Gregory, L., Lam, W.Y., O'Neill, C.M., et al. (2014). Cell-intrinsic lysosomal lipolysis is essential for alternative activation of macrophages. Nat. Immunol. *15*, 846–855.

Huh, J.Y., Kim, J.I., Park, Y.J., Hwang, I.J., Lee, Y.S., Sohn, J.H., Lee, S.K., Alfadda, A.A., Kim, S.S., Choi, S.H., et al. (2013). A novel function of adipocytes in lipid antigen presentation to iNKT cells. Mol. Cell. Biol. *33*, 328–339.

Humphries, F., and Moynagh, P.N. (2015). Molecular and physiological roles of Pellino E3 ubiquitin ligases in immunity. Immunol. Rev. *266*, 93–108.

Jeon, Y., Ko, E., Lee, K.Y., Ko, M.J., Park, S.Y., Kang, J., Jeon, C.H., Lee, H., and Hwang, D.S. (2011). TopBP1 deficiency causes an early embryonic lethality and induces cellular senescence in primary cells. J. Biol. Chem. *286*, 5414–5422.

Jin, W., Chang, M., and Sun, S.C. (2012). Peli: a family of signal-responsive E3 ubiquitin ligases mediating TLR signaling and T-cell tolerance. Cell. Mol. Immunol. *9*, 113–122.

Krausgruber, T., Blazek, K., Smallie, T., Alzabin, S., Lockstone, H., Sahgal, N., Hussell, T., Feldmann, M., and Udalova, I.A. (2011). IRF5 promotes inflammatory macrophage polarization and TH1-TH17 responses. Nat. Immunol. *12*, 231–238.

Lawrence, T., and Natoli, G. (2011). Transcriptional regulation of macrophage polarization: enabling diversity with identity. Nat. Rev. Immunol. *11*, 750–761.

Lumeng, C.N., Bodzin, J.L., and Saltiel, A.R. (2007). Obesity induces a phenotypic switch in adipose tissue macrophage polarization. J. Clin. Invest. *117*, 175–184.

Moynagh, P.N. (2014). The roles of Pellino E3 ubiquitin ligases in immunity. Nat. Rev. Immunol. *14*, 122–131.

Murray, P.J., Allen, J.E., Biswas, S.K., Fisher, E.A., Gilroy, D.W., Goerdt, S., Gordon, S., Hamilton, J.A., Ivashkiv, L.B., Lawrence, T., et al. (2014). Macrophage activation and polarization: nomenclature and experimental guidelines. Immunity *41*, 14–20.

Negishi, H., Ohba, Y., Yanai, H., Takaoka, A., Honma, K., Yui, K., Matsuyama, T., Taniguchi, T., and Honda, K. (2005). Negative regulation of Toll-like-receptor signaling by IRF-4. Proc. Natl. Acad. Sci. USA *102*, 15989–15994.

O'Neill, L.A., and Pearce, E.J. (2016). Immunometabolism governs dendritic cell and macrophage function. J. Exp. Med. *213*, 15–23.

Ordureau, A., Smith, H., Windheim, M., Peggie, M., Carrick, E., Morrice, N., and Cohen, P. (2008). The IRAK-catalysed activation of the E3 ligase function of Pellino isoforms induces the Lys63-linked polyubiquitination of IRAK1. Biochem. J. *409*, 43–52.

Ren, J., Chen, X., and Chen, Z.J. (2014). IKKβ is an IRF5 kinase that instigates inflammation. Proc. Natl. Acad. Sci. USA *111*, 17438–17443.

Saigusa, R., Asano, Y., Taniguchi, T., Yamashita, T., Ichimura, Y., Takahashi, T., Toyama, T., Yoshizaki, A., Sugawara, K., Tsuruta, D., et al. (2015). Multifaceted contribution of the TLR4-activated IRF5 transcription factor in systemic sclerosis. Proc. Natl. Acad. Sci. USA *112*, 15136–15141.

Sica, A., and Bronte, V. (2007). Altered macrophage differentiation and immune dysfunction in tumor development. J. Clin. Invest. *117*, 1155–1166.

Sica, A., and Mantovani, A. (2012). Macrophage plasticity and polarization: in vivo veritas. J. Clin. Invest. *122*, 787–795.

Tannahill, G.M., Curtis, A.M., Adamik, J., Palsson-McDermott, E.M., McGettrick, A.F., Goel, G., Frezza, C., Bernard, N.J., Kelly, B., Foley, N.H., et al. (2013). Succinate is an inflammatory signal that induces IL-1β through HIF-1α. Nature *496*, 238–242.

Torres-Castro, I., Arroyo-Camarena, U.D., Martinez-Reyes, C.P., Gomez-Arauz, A.Y., Duenas-Andrade, Y., Hernandez-Ruiz, J., Bejar, Y.L., Zaga-Clavellina, V., Morales-Montor, J., Terrazas, L.I., et al. (2016). Human monocytes and macrophages undergo M1-type inflammatory polarization in response to high levels of glucose. Immunol. Lett. *176*, 81–89.

Van Rooijen, N., and Sanders, A. (1996). Kupffer cell depletion by liposome-delivered drugs: comparative activity of intracellular clodronate, propamidine, and ethylenediaminetetraacetic acid. Hepatology *23*, 1239–1243.

Weiss, M., Byrne, A.J., Blazek, K., Saliba, D.G., Pease, J.E., Perocheau, D., Feldmann, M., and Udalova, I.A. (2015). IRF5 controls both acute and chronic inflammation. Proc. Natl. Acad. Sci. USA *112*, 11001–11006.

Xiao, Y., Jin, J., Chang, M., Chang, J.H., Hu, H., Zhou, X., Brittain, G.C., Stansberg, C., Torkildsen, Ø., Wang, X., et al. (2013). Peli1 promotes microglia-mediated CNS inflammation by regulating Traf3 degradation. Nat. Med. *19*, 595–602.

Yang, S., Wang, B., Humphries, F., Hogan, A.E., O'Shea, D., and Moynagh, P.N. (2014). The E3 ubiquitin ligase Pellino3 protects against obesity-induced inflammation and insulin resistance. Immunity *41*, 973–987.